Available online at www.sciencedirect.com
ScienceDirect
Trans. Nonferrous Met. Soc. China 24(2014) 2072−2078
Transactions of Nonferrous Metals Society of China
www.tnmsc.cn

Influence of dispersoids on grain subdivision and texture evolution in aluminium alloys during cold rolling

Qing-long ZHAO, Bjørn HOLMEDAL

Department of Materials Science and Engineering, Norwegian University of Science and Technology, Trondheim N-7491, Norway

Received 17 October 2013; accepted 4 April 2014

Abstract: Al−Mn alloys containing similar amounts of solutes but various dispersoid densities were cold rolled. The grain subdivision and micro-texture were examined by electron backscatter diffraction and orientation imaging microscopy. Macro-texture was measured by X-ray diffraction. It is found that a high density of fine dispersoids enhances the development of the copper and *S* textures at large strains (~3), and also induces a higher fraction of high-angle grain boundaries. At smaller strains, the texture and high-angle grain boundaries are not evidently influenced by the density of dispersoids. It is suggested that the texture evolution, which is enhanced by dispersoid pinning effect, contributes to the grain subdivision and the formation of high-angle grain boundaries.

Key words: aluminium alloys; grain boundary; texture; deformation; microstructure

1 Introduction

The deformation structure of fcc metals, mainly Cu, Ni and Al, has been investigated in a number of studies [1−4]. While coarse particles induce the formation of deformation zones containing large local misorientation gradients [5], fine particles enhance the tendency for dislocations to arrange into a cell structure [6], leading to a reduced cell size [1,6]. Besides, dispersoids affect the grain subdivision during deformation [7]. The evolution of high-angle grain boundaries (HAGB) and grain refinement mechanisms during deformation at large strain has received much attention in recent research, since severe plastic deformation (SPD) was used to produce nanocrystalline materials. The influence of non-shearable fine dispersoids on misorientation across boundaries reported in previous research seems controversial. It was reported that fine-dispersed particles increased effectively the mean misorientation between subgrains [8], and also the misorientation of cell block walls [9]. Conversely, a lower misorientation across subgrains [7,10] and diffuse boundaries [7] due to dispersoids and also a smaller long-range orientation spread [10] were reported, compared to a single-phase alloy. Previous research shows that the HAGB fraction was reduced by a high density of dispersoids at very large strains (von Mises strain >3) [7,9]. The influence of dispersoids at smaller strains is contradictory, where both a small increase and decrease in HAGB fraction of dispersed alloys were reported [7,9]. A very high HAGB fraction (60%−70%) at von Mises strain of 1−3 was reported due to the presence of dispersoids [8].

It is generally agreed that dispersoids reduce the average slip length and result in a homogeneous (Taylor) deformation/slip pattern [7,8,10,11]. Therefore, the deformation is relatively homogeneous compared to the heterogeneous deformation in coarse-grain single-phase alloys (containing plenty of micro-/macro-shear bands). The critical slip length necessary to achieve a homogeneous deformation is not known yet. The previous research [7,8] compared alloys containing dispersoids with a single-phase alloy. The slip patterns and grain subdivision mechanisms were found to be different: a homogeneous slip pattern in the alloys containing dispersoids and a heterogeneous slip pattern in the coarse-grain single-phase alloys. The heterogeneous slip pattern in coarse-grain single-phase alloys leads to the formation of intense microshear bands [3], which is a mechanism reported to form

Foundation item: Project supported by the Research Council of Norway, Hydro and Sapa Technology Under the Project MOREAL
Corresponding author: Qing-long ZHAO; Tel: +47-73596785; E-mail: qinglong.zhao@gmail.com
DOI: 10.1016/S1003-6326(14)63314-8

HAGBs [7,12]. The spacing of micro-shear bands decreases rapidly and the misorientation across micro-shear band walls increases dramatically with increasing strain at medium and large strains [3]. APPS et al [7] claimed that the fine dispersoids inhibited the formation of microshear bands during deformation so that the rate of high-angle grain boundary generation was reduced at low to medium strains. However, their results showed that the HAGB fraction in the alloy containing dispersoids was a bit higher than that in the single-phase alloy at strains smaller than 3. *S*-bands, which are a transitional structure to a lamellar structure at large strains and another mechanism of grain subdivision [13], were also observed in alloys containing dispersoids at medium strains [9,14].

The deformation structure of single-phase materials has been investigated for years, especially by the severe plastic deformation recently. However, comparisons between dispersed alloys with various dispersoid densities and well-controlled solute levels were rarely reported. The effect of dispersoids on grain subdivision and texture evolution will be investigated in this work.

2 Experimental

The material used in this work was an Al−Mn−Fe−Si direct chill cast billet produced by Hydro Aluminium. The nominal chemical composition (mass fraction, %) of the alloy was: Mn 0.97, Fe 0.50, Si 0.15 and others 0.05. The average grain size of the material was ~100 μm. Homogenization treatments in an air circulation furnace were carried out to achieve two dispersoid distributions with the similar solute contents. Sample BH was heated from room temperature (RT) to 723 K and held for 4 h. Sample BL was heated from RT to 873 K and held for 4 h, and then cooled in a rate of 25 K/h to 773 K and held for 4 h. The heating rate was 50 K/h. The samples BH and BL were rolled at room temperature in a laboratory mill down to about 1.5 mm in thickness to achieve the von Mises strains of 0.74, 1.8, and 3.3 (nominal reduction 50%, 80%, and 95% respectively). The as-homogenized microstructure and deformation structure were observed by backscattered electron channeling contrast (BSE-ECC) imaging at 15 kV in a Zeiss Ultra 55 field emission gun scanning electron microscope (SEM) equipped with an electron backscatter diffraction (EBSD) detector. The EBSD data were processed by TSL OIM software of EDAX Company.

Similar solute contents in BH and BL were achieved by homogenization treatments, indicated by the similar electrical conductivities. The coarse constituent particles, α-Al(Mn,Fe)Si and Al_6(Mn,Fe), formed at dendrite and grain boundaries during casting. The particles became coarser and spheroidized during homogenization at a high temperature. Dispersoids, α-Al(Mn,Fe)Si and Al_6(Mn,Fe) precipitated during the homogenization. Precipitate free zones (PFZs) around dendrite and grain boundaries were observed in BL, and the area fraction of PFZs was ~42%. The details of microstructure characterization can be referred to Ref. [15], and a summary of previous results is listed in Table 1.

Table 1 Microstructural parameters

Sample	Electrical Conductivity/ ($MS\cdot m^{-1}$)	Constituent particle		Dispersoid	
		Size/ μm	Area fraction/%	Size/ μm	Spacing/ μm
BH	24.0	1.0	2.4	0.11	0.9
BL	23.8	1.3	2.8	0.16	1.4

3 Results

The subgrain structure after rolling was observed by SEM, as shown in Fig. 1. The threshold misorientation detected in EBSD was set to 2° to eliminate excessive misorientation noise, so the misorientation of sub-boundaries (or low-angle boundaries, LAB) was defined to be 2°−15°. The high-angle grain boundaries (HAGB) are higher than 15°. Two types of EBSD scanning were carried out for alloys at a strain of 1.8 (small area containing very few constituent particles with a step size of 50 nm; large area of a step size of 500 nm). The small step size produces a better resoltution of LAB, which are used in Table 2. The large area scans give a better statistical result, used for misorientation

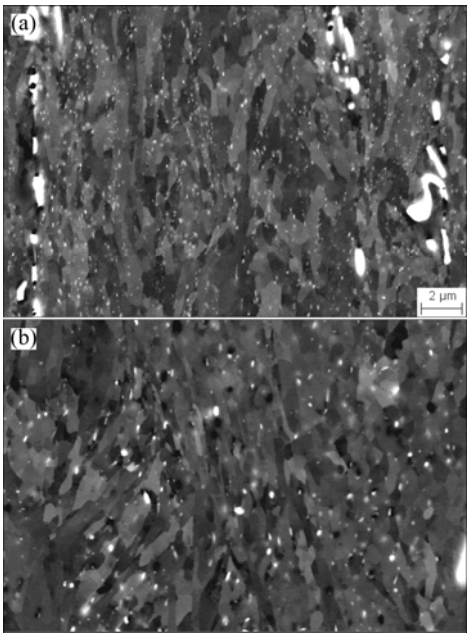

Fig. 1 SEM backscattered electron images of subgrain structure and dispersoids at a strain of 1.8 (at same magnification): (a) BH; (b) BL

Table 2 Average boundary misorientation, HAGB length fraction, HAGB length per area, and HAGB spacing along ND

Sample	von Mises strain	Misorientation/(°)		HAGB fraction	HAGB length per area/ μm^{-1}	HAGB spacing/ μm
		LAB	HAGB			
BH	1.8	4.2*	39.3 (45.8*)	0.22	0.19	6.9
BL	1.8	4.6*	37.8 (43.7*)	0.24	0.22	6.3
BH	3.3	5.0	42.8	0.36	1.63	0.7
BL	3.3	5.1	39.2	0.26	1.12	1.1

*small scanning areas containing very few constituent particles with a step size of 50 nm

distributions in Fig. 2 and micro-textures in Fig. 3(b). The scanned area at a strain of 3.3 always contained constituent particles due to the large strain, and the step size was 40 nm.

The mean misorientations of LAB were similar for BH and BL at large strains (Table 2), and the distributions of LAB as well (Fig. 2), indicating that the dispersoids had little influence on the misorientations across sub-boundaries. The mean misorientation of HAGB in BH at a strain of 3.3 was higher than that in BL (Table 2), and the misorientation frequency distribution (Fig. 2) shows that BH had a higher fraction of HAGB than BL at very high misorientation angles (>45°). The HAGB fraction, which is frequently used in the study on grain refinement, was calculated from the misorientation frequency distribution. However, the HAGB fraction is sensitive to the distribution of LAB, especially the detection of very low angle boundaries. Thus, the HAGB length per area, L_A, is used as a supplement to the HAGB fraction, because HAGB length per area can be measured directly by EBSD. The value of L_A is an overestimate of the real value due to the square grid used in EBSD maps [16], but the correction is not necessary since it does not affect the comparison here. The grain size and HAGB spacing are proportional to the inverse of the HAGB length per area. The HAGB fraction and HAGB length per area in BH at a strain of 3.3 were significantly higher than those in BL, suggesting that grain subdivision was promoted in BH at large strains.

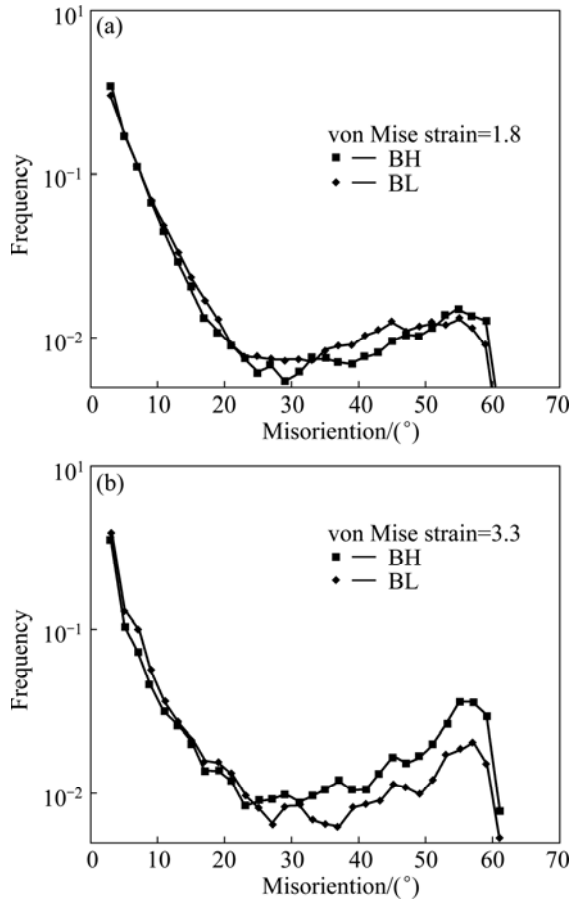

Fig. 2 Frequency distributions of boundary misorientation

The macro-textures of the cold rolled alloys were measured by X-ray diffraction (XRD), showing a strong β-fiber texture (Fig. 3(a)). The maximum intensity in each φ_2 (phi2) section is plotted in Fig. 3, since the location of the measured β-fiber may vary from the ideal fiber. The φ_2=0 and φ_2=45º sections of ODF are also illustrated in Fig. 3(c), showing the locations of deformation textures in ODF. The macro-textures of BH and BL were similar at a medium strain (0.7). The copper {112} ⟨111⟩ texture component became stronger in BH as the strain increased to 1.8 and above, and the S {123} ⟨634⟩ texture also became prominent in BH at a large strain (3.3). The micro-textures of the EBSD scanning areas, where boundary misorientations were measured, are shown in Fig. 3(b). The micro-textures at a strain of 1.8 (with a step size of 500 nm) were different from the macro-textures measured by XRD. This is because the EBSD collects crystallographic information locally. The other micro-textures were qualitatively similar to their corresponding macro-textures, despite of the different intensities.

4 Discussion

4.1 Evolution of high-angle grain boundaries and textures

The HAGB fraction and HAGB length per area of BH at large strains are found to be significantly higher than those of BL, indicating that the grain refinement (or subdivision) was promoted in the presence of a high density of dispersoids in BH at high strain. The mechanism, which promotes the grain refinement in BH at a strain of 3.3, will be discussed in this section. HUGHES and HANSEN [12] investigated grain subdivision mechanisms. They distinguished the

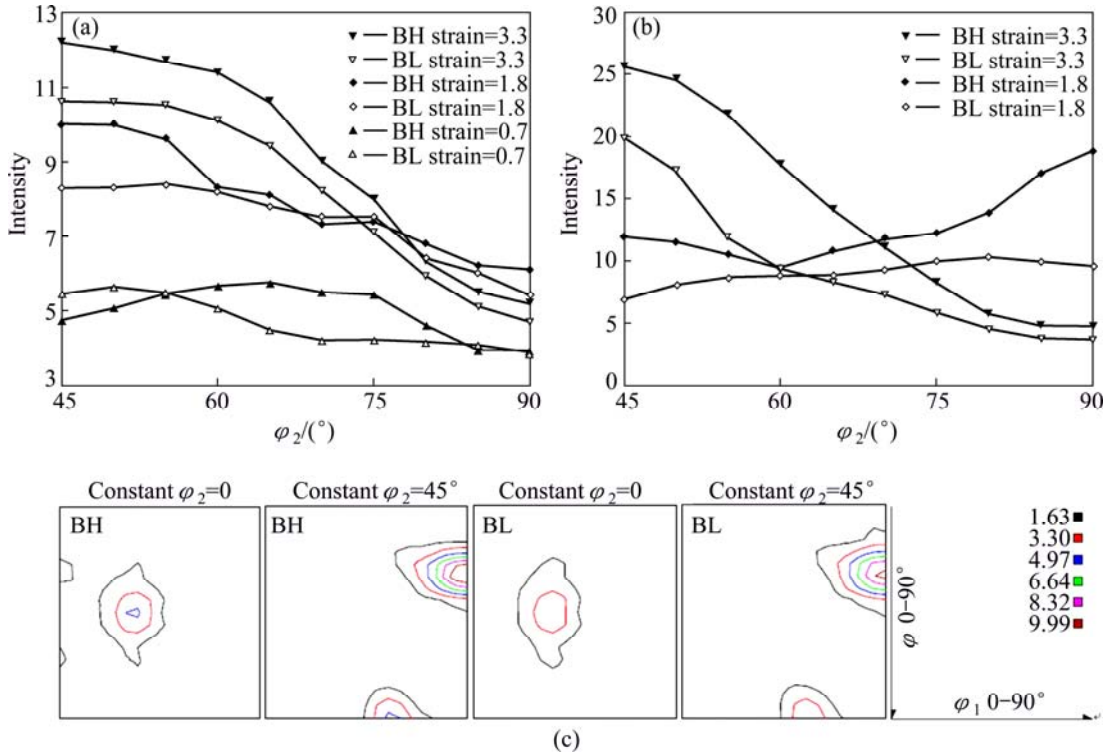

Fig. 3 Macro-textures measured by X-ray diffraction (a), micro-textures measured by EBSD (b) and selected sections of ODF measured by X-ray diffraction at a strain of 3.3 (c)

subdivision mechanisms due to the formation of cell blocks, *S*-bands, microshear bands and shear bands, and studied the influence of texture evolution as well. Uniformly distributed large particles were reported to enhance the grain refinement effectively at medium and large strains (von Mises strain 1−4) [17].

The large particles in this work are initially heterogeneously distributed, concentrated at grain boundaries and dendrite arm boundaries. The volume fractions of large particles were very similar in BH and BL. Thus, the effect of constituent particles on the grain refinement is expected to be small when comparing BH and BL. Moreover, the large particles were reported to promote the grain refinement significantly at a strain of 1−2, and to increase the fraction of HAGB in the entire angle range of HAGB [17]. No significant difference between BH and BL in HAGB fraction and misorientation angle distribution is found at a strain of 1.8 in this work. It suggests that the higher degree of grain refinement of BH at high strains cannot be attributed to the effect of coarse particles.

Cell block formation leads to HAGBs which are generally less than 35° [12]. The formation of HAGBs related to texture evolution usually occurs in a higher angle range (>40°) than other grain subdivision mechanisms, e.g., *S*-bands [12]. APPS et al [7] have reported that dispersoids inhibit the formation of micro-shear bands during deformation. Figure 2 shows that the misorientation distribution of HAGBs at a strain of 3.3 has a peak in the range higher than 40°, where BH had a higher fraction of HAGB than BL. The HAGB fraction increased significantly in BH, while the misorientation distribution of LAB changed little. It implies that the high HAGB fraction in BH is not due to the increase in misorientations of cell blocks, but rather related to the texture evolution according to Ref. [12].

Figure 4 illustrates the substructure of BH at a strain of 3.3, demonstrating the grain subdivision related to texture evolution. Line A in Fig. 4 contains subdivided grains with several texture components. Line A crosses 13 texture bands, including 9 HAGBs, and another 4 LABs of 11°−15° (Fig. 5), which would probably become HAGB at larger strains. The initial grain size is ~100 μm, so after the reduction rate of 95%, the geometrical grain size along ND is ~5 μm if no subdivision occurs. Line A probably crosses only one or two original HAGBs. Thus, most of HAGBs are formed by grain subdivision related to texture evolution. The grain subdivision depends strongly on the initial orientation [18,19]. The ambiguity of the selections of slip systems for the unstable orientations leads to diverging rotations within a grain, i.e., grain subdivisions, resulting in more HAGBs. The stable orientations during rolling are *β*-fiber orientations in Euler space, especially the copper orientation [20]. The grains of stable orientations have a small tendency to subdivide due to

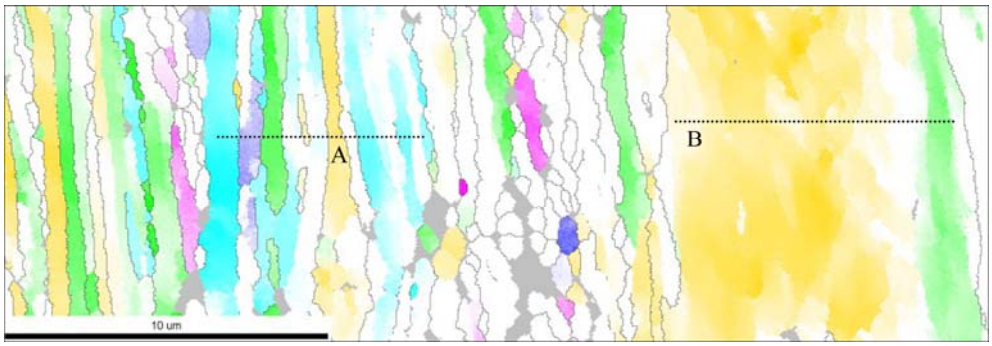

Fig. 4 Structure of BH at a strain of 3.3, illustrating distributions of micro-textures and grain subdivision (Noise points are in grey; high-angle grain boundaries black lines. Several texture components are in colour, i.e., copper {112}⟨111⟩, *S* {123}⟨634⟩, Goss {011}⟨100⟩, brass {110}⟨112⟩, and {025}⟨100⟩. Maximum deviation from ideal orientation is 12°

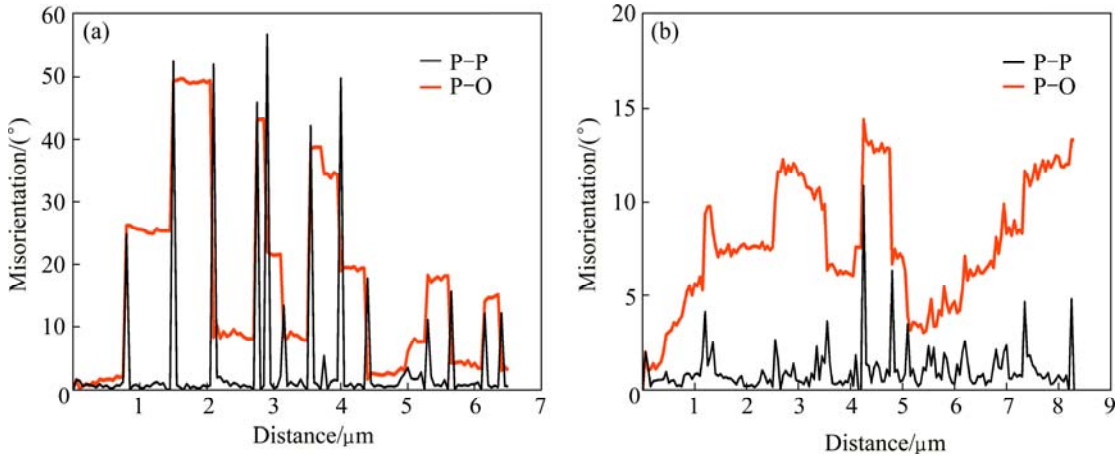

Fig. 5 Misorientation profile along line A (a) and along line B (b) in Fig. 4 (P−P shows the misorientations between adjacent points, P−O shows the misorientations compared to the original point.)

texture [18,19]. Line B demonstrates the inhibited subdivision in a grain of a stable orientation (probably the copper texture). The large grain in line B contains only two texture bands, i.e., the copper and the *S* texture components, but no HAGBs. It suggests that the tendency of subdivision is small in grains of stable orientations. APPS et al [7] reported that weakly misorientated and diffused boundaries were present at strains of 2−3 in a dispersoid-containing alloy. This is probably related to local orientations and the different deformation mode, i.e., the influence of equal channel angular extrusion on structure and texture is very different from that of rolling in the present work. The grain of the stable orientation (line B) has a large orientation gradient within the grain and weakly misorientated boundaries (Fig. 5). However, the transition between texture bands is sharp in line A, and the orientation gradient within each texture band is small (Fig. 5).

The promoted grain subdivision in alloys with the high density of dispersoids is ascribed to the texture evolution. The texture evolution is not specified in previous research [7, 9], so a quantitative comparison with previous research is impossible. The previous research [9] compared alloys containing different density of dispersoids. The high density of dispersoids results in more dislocation accumulation at small strains, leading to higher mean misorientation of cell boundaries if the cell sizes are similar [9]. The similar HAGB fractions of dispersed alloys at large strains in Ref. [9] are probably caused by a fact that the high density of precipitates affects the texture evolution more than the low density of dispersoids.

4.2 Effect of dispersoids on texture evolution

The texture intensity of BH and BL is relatively weak due to the randomization effect of large constituent particles [21]. However, it is evident that the copper texture component has become stronger in the alloy with a high density of dispersoids (BH) at large strains in Fig. 3. It has been reported that non-shearable particles increased the sharpness of the copper texture component [11,21]. They suggested that the dispersoid effect on texture was caused by a reduction in the free travelling

path of dislocations, and this effect was similar to reducing the initial grain size, which also enhances *β*-fiber textures. Reducing the initial grain size enhances *β*-fiber textures at medium strains but the effect diminishes at large strains [22]. The dispersoids, by contrast, do not affect significantly the intensities of *β*-fiber textures at medium strains, but enhance the copper and *S* textures at large strains (Fig. 3). The slip length of dislocations is not expected to be affected by dispersoids at large strains since most of the dispersoids are trapped in boundaries.

It has been noted that deformation textures of alloys containing dispersoids are closer to the prediction by the full constraint (FC) Taylor model, rather than that of the relaxed constraint (RC) Taylor model [11]. Dispersoids pin the boundaries, inducing stronger boundary constraints to grain deformation. Hence, the textures show a strong copper and *S* texture, as predicted by FC-Taylor model. An early work [23] has shown that the simulated *β*-fiber of FC Taylor model was not evidently different from that of RC Taylor model at small strains, but it became significantly stronger at large strains. This is qualitatively consistent with the texture evolution in this work. The texture evolution due to dispersoids would probably slow down at very large strains, so the HAGB induced by texture would be minor in newly broken grains.

5 Conclusions

The presence of dispersoids enhances the development of copper and *S* texture at large strains. It is suggested that it is because dispersoids pin sub-boundaries, leading to a deformation more similar to the one predicted by the full constraint Taylor model. The HAGB fractions are similar at small strains, but at a strain of ~3, a higher HAGB fraction is found in the alloy containing a high-density of dispersoids than in the one containing a low-density of dispersoids. The texture evolution affects the grain subdivision and contributes to the formation of HAGB.

Acknowledgement

The authors are grateful for the helpful discussion with Yan-jun LI at SINTEF. This work was funded by the Research Council of Norway, Hydro and Sapa Technology under the project MOREAL.

References

[1] LLOYD D J, KENNY D. The structure and properties of some heavily cold worked aluminum alloys [J]. Acta Metallurgica, 1980, 28(5): 639−649.

[2] BAY B, HANSEN N, HUGHES DA, KUHLMANN-WILSDORF D. Overview no. 96: Evolution of f.c.c. deformation structures in polyslip [J]. Acta Metallurgica et Materialia, 1992, 40(2): 205−219.

[3] HURLEY P J, HUMPHREYS F J. The application of EBSD to the study of substructural development in a cold rolled single-phase aluminium alloy [J]. Acta Materialia, 2003, 51(4): 1087−1102.

[4] HUANG X, WINTHER G. Dislocation structures. Part I. Grain orientation dependence [J]. Philosophical Magazine, 2007, 87(33): 5189−5214.

[5] HUMPHREYS F J. Local lattice rotations at second phase particles in deformed metals [J]. Acta Metallurgica, 1979, 27(12): 1801−1814.

[6] BARLOW C Y, HANSEN N. Deformation structures in aluminium containing small particles [J]. Acta Metallurgica, 1989, 37(5): 1313−1320.

[7] APPS P J, BERTA M, PRANGNELL P B. The effect of dispersoids on the grain refinement mechanisms during deformation of aluminium alloys to ultra-high strains [J]. Acta Materialia, 2005, 53(2): 499−511.

[8] BARLOW C Y, HANSEN N, LIU Y L. Fine scale structures from deformation of aluminium containing small alumina particles [J]. Acta Materialia, 2002, 50(1): 171−182.

[9] CABIBBO M, EVANGELISTA E. A TEM study of the combined effect of severe plastic deformation and (Zr), (Sc+Zr)-containing dispersoids on an Al−Mg−Si alloy [J]. Journal of Materials Science, 2006, 41(16): 5329−5338.

[10] HUMPHREYS F J, HATHERLY M. Recrystallization and related annealing phenomena [M]. Amsterdam: Elsevier, 2004: 55.

[11] ENGLER O, HIRSCH J, LÜCKE K. Texture development in al 1.8wt% Cu depending on the precipitation state—I. Rolling textures [J]. Acta Metallurgica, 1989, 37(10): 2743−2753.

[12] HUGHES D A, HANSEN N. High angle boundaries formed by grain subdivision mechanisms [J]. Acta Materialia, 1997, 45(9): 3871−3886.

[13] HUGHES D A, HANSEN N. Microstructural evolution in nickel during rolling from intermediate to large strains [J]. Metallurgical Transactions A, 1993, 24(9): 2022−2037.

[14] YAO Z Y, ZHANG Z Q, GODFREY A, LIU W, LIU Q. Microstructure and texture evolution of particle-containing AA3104 alloy cold rolled to large strains [J]. Materials Science and Technology, 2010, 26(5): 539−546.

[15] ZHAO Qing-long, HOLMEDAL B, LI Yan-jun. Influence of dispersoids on microstructure evolution and work hardening of aluminium alloys during tension and cold rolling [J]. Philosophical Magazine, 2013, 93(22): 2995−3011.

[16] CAO W Q, GODFREY A, LIU Q. EBSP investigation of microstructure and texture evolution during equal channel angular pressing of aluminium [J]. Materials Science and Engineering A, 2003, 361(1−2): 9−14.

[17] APPS P J, BOWEN J R, PRANGNELL P B. The effect of coarse second-phase particles on the rate of grain refinement during severe deformation processing [J]. Acta Materialia, 2003, 51(10): 2811−2822.

[18] RAABE D, ZHAO Z, MAO W. On the dependence of in-grain subdivision and deformation texture of aluminum on grain interaction [J]. Acta Materialia, 2002, 50(17): 4379−4394.

[19] DELANNAY L, MISHIN O V, JENSEN D J, VAN HOUTTE P. Quantitative analysis of grain subdivision in cold rolled aluminium [J]. Acta Materialia, 2001, 49(13): 2441−2451.

[20] ZHOU Y, TÓTH L S, NEALE K W. On the stability of the ideal orientations of rolling textures for f.c.c. polycrystals [J]. Acta Metallurgica et Materialia, 1992, 40(11): 3179−3193.

[21] LÜCKE K, ENGLER O. Effects of particles on development of microstructure and texture during rolling and recrystallisation in fcc alloys [J]. Materials Science and Technology, 1990, 6(11): 1113−1130.

[22] HANSEN N, BAY B, JENSEN D J, LEFFERS T. Effect of grain size

on the microstructure and texture of cold-rolled aluminium [C]//The 7th International Conference on the Strength of Metals and Alloys. Montreal. 1985: 317−322.

[23] HIRSCH J, LÜCKE K. Overview no. 76: Mechanism of deformation and development of rolling textures in polycrystalline fcc metals—II. Simulation and interpretation of experiments on the basis of taylor-type theories [J]. Acta Metallurgica, 1988, 36: 2883−2904.

弥散相对铝合金冷轧过程中晶粒分裂和织构演变的影响

赵庆龙，Bjørn HOLMEDAL

Department of Materials Science and Engineering, Norwegian University of Science and Technology, Trondheim N-7491, Norway

摘　要：制备了 2 种含有相近合金元素含量但不同的弥散第二相密度的铝锰合金冷轧板材。利用背散射电子衍射和取向成像图技术研究了晶粒分裂和微观织构，使用 X 射线衍射技术测量了宏观织构。研究发现当应变达到 3 左右时，高密度的小尺寸弥散相会促进铜型和 *S* 型织构的形成，同时增加了大角晶界所占比例。在小应变下，弥散相对织构和大角晶界的影响不显著。研究显示弥散相通过钉扎晶界从而促进织构演化，进而影响晶粒分裂和大角晶界的形成。

关键词：铝合金；晶界；织构；变形；微观组织

(Edited by Yun-bin HE)